

Interphase behaviour in graphite-thermoplastic monofilament composites

Part II *Cyclic behaviour*

L. S. SCHADLER*, C. LAIRD

Department of Materials Science and Engineering, University of Pennsylvania, Philadelphia, PA 19139, USA

J. C. FIGUEROA

E.I. Du Pont de Nemours and Co. Inc, Experimental Station, PO Box 80304, Wilmington, DE 19880-0304, USA

The fatigue properties of continuous filament composites are dependent on the fibre-matrix interphase behaviour, specifically the ability of the interphase to transfer load durably from the matrix to the fibre, and the energy dissipated in the interphase during crack growth. Although there has been a large effort to understand interphase behaviour in order to tailor the interphase for specific bulk composite properties, the basic role of the interphase in cyclic fatigue is not well understood. A monofilament composite system of a carbon fibre in a thermoplastic matrix was employed to study the behaviour of the fibre/matrix interphase during cycling because fibre/fibre interaction and processing variability are eliminated. The effects of cyclic loading direction, frequency and amplitude were studied with an optical fragmentation technique. Damage was characterized by fibre-matrix debonding, a reduction of the average interphase shear stress determined by the fragmentation test, and changes in the locus of failure as determined by SEM fractography. It was found that the integrity of the interphase was matrix dominated, and frequency dependent, and was not affected by the initial strength of the interphase when the cyclic loading was transverse to the fibre direction. When the composite was subjected to axial cyclic loading, the damage was dominated by the strength of the fibre until the fibre failed. After fibre failure, the subsequent damage was matrix dominated.

1. Introduction

Continuous fibre-reinforced thermoplastic matrix composites are becoming increasingly important engineering materials because thermoplastics can be extrusion moulded, can be remelted and remoulded for in-the-field repairs, are less hygroscopic than most thermosets, and some thermoplastics can maintain their mechanical properties at high temperatures [1].

The crack growth resistance of a composite depends on the properties of the interphase (defined as the region beginning at the point in the fibre where the properties differ from that of the bulk fibre, and ending at the point in the matrix where the properties become equal to that of the bulk matrix). A strong interphase will often result in a brittle composite fracture because the crack cannot be diverted around the fibres; a weak interphase can lead to a tougher composite because the interphase tends to divert a crack along the interphase, and energy can be absorbed in both extending the crack, and in fibre pull-out [2]. If the properties of the interphase change with loading history, the crack growth resistance of a composite will change; the

integrity of the interphase and the load-transfer behaviour have been shown to change [3, 4]. An understanding of the interphase behaviour in cyclic fatigue is thus essential to understanding bulk composite fatigue behaviour.

Previous work investigated the monotonic behaviour of AU4/thermoplastic mono-filament composites, and the effect of surface energy, surface morphology, and matrix on the interphase behaviour using a variation of the critical length fragmentation technique [5, 6]. In the present experimental investigation the cyclic behaviour of the interphase in AU4/polycarbonate (PC) mono-filament composites was studied. The effects of strain rate, loading direction, amplitude, and initial interphase properties were investigated.

2. Experimental procedure

Part I of this report described the sample preparation technique, and the optical fragmentation technique,

* To whom correspondence should be addressed at IBM T. J. Watson Research Center, PO Box 218, Yorktown Heights, NY 10598, USA.

termed the lambda technique, for measuring the average interphase shear stress (ISS) (the ability of the interphase to transfer load from the matrix to the fibre) [5].

In order to measure the effect of the interphase on the fatigue behaviour, the interphase was altered using a plasma etch. As reported in Part I, the plasma etch altered the surface energy, the surface roughness, and the average ISS. The effect of plasma etching on these parameters is summarized in Fig. 1. As the fibre surface was treated, the surface roughened, reaching a maximum roughness after 3 min of treatment; the surface energy increased due to treatment, and reached a plateau after 1 min of treatment; the average ISS peaked after 3 min of treatment. The conclusion from the report was that the increase in the average ISS was due to an increased surface roughness that increased the average interphase shear stress (ISS) through a mechanism of improved micromechanical interlocking.

For this investigation, three treatment times were chosen in order to study the effect of the interphase on the fatigue behaviour: (1) as-received fibres, (2) fibres treated for 1 min chosen because the surface energy had increased but the average ISS had not, and (3) fibres treated for 3 min chosen because the surface roughness, surface energy, and average ISS were all at a maximum.

2.1. Fatigue tests

Fatigue tests were carried out in both the transverse and axial direction on model mono-filament composites. The transverse samples will be discussed first.

In order to eliminate any effects of moulding or treatment batch, each moulding used for fatigue was cut in half such that half of each fibre remained in each half of the mould. One half of the mould was cycled, and the other was not. After cycling, the lambda fragmentation test and subsequent average ISS calculations were done for both the non-cycled and the cycled half of the mould, so that the behaviour of one-half of a fibre was compared to that of the other half.

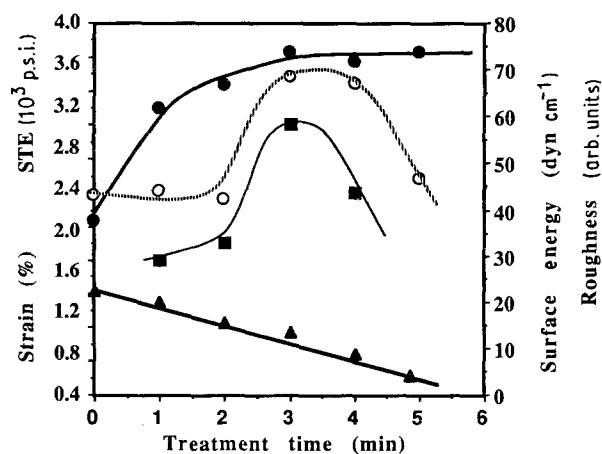


Figure 1 The fibre surface roughness, fibre surface energy, and the interphase average shear stress as a function of treatment time. (■) Roughness, (▲) minimum failure strain, (○) STE, (●) surface energy.

The transverse samples measured 65 mm × 90 mm × 0.5 mm. Each sample contained six fibres: two of each treatment time, as-received, 1 min, and 3 min.

Because PC yields at 7%, but remains fairly linear below 3%, strain amplitudes in the low range of 2%–2.7% for transverse cyclic tests were employed to minimize damage in the bulk matrix, but to allow for some damage in the interphase region due to stress concentrations. Samples were tested at a range of frequencies, and a range of cycles as shown in Table I.

The dimensions of the axial fatigue samples measured 30 mm × 90 mm × 0.5 mm. As-received fibres, and fibres treated for 3 min were tested at several amplitudes.

Fatigue tests were carried out on an Instron 1331 servohydraulic fatigue machine. Tests were run under load control with $R = 0.1$. Creep during testing was less than 5% of the total strain, and the change in residual modulus was small. The wave form was triangular to maintain a constant loading rate during the test.

2.2 Scanning electron microscopy

Fibres were viewed in the SEM by pulling fibres from the matrix using the method described in Part I [5]. Fibres were viewed before and after cycling, and the failure surfaces were examined to help determine whether the locus of interphase failure was in the matrix portion of the interphase, the fibre portion, or directly along the fibre–matrix two-dimensional interface.

3. Results

The results of transverse fatigue will be presented first including: (1) the state of stress in the interphase during cycling, (2) a qualitative overview of damage at each strain amplitude, (3) strain-rate effects, and (4) the effect of cycles on damage to the interphase. The behaviour of the AU4/PC interphase when the composite is fatigued axially, is presented last.

Damage due to fatigue was defined quantitatively as the reduction in the average ISS measured for the

TABLE I Loading schedule for the transverse cyclic tests

Cyclic strain (%)	Frequency (Hz)	Cycles					
		100	500	1000	3000	5000	10000
2.0	0.01			•			
	0.05	•		•	•	•	•
	0.1			•		•	•
	0.5					•	
	1.0			•		•	•
2.35	0.01	•		•			
	0.05	•	•	•	•	•	
	0.1		•	•		•	
	0.5			•		•	•
	1.0			•		•	•
2.7	0.01			•			
	0.1			•			
	1.0			•		•	

AU4/PC composite using the lambda technique, and qualitatively as the difference in the photoelastic patterns surrounding a fibre break in non-cycled and cycled samples, and changes in the locus of failure as seen in SEM fractographs.

3.1. Transverse fatigue

3.1.1. Residual strain

An understanding of the stress state in the interphase region during transverse cycling is important in order to analyse the behaviour of the interphase. The stress state in the region surrounding the fibre was solved in closed form for both the residual moulding stresses and then for the additional stresses induced by loading the sample in the transverse direction. Fig. 2 shows: (1) the radial and hoop moulding stress components as a function of radial distance from the fibre centre, and (2) the radial and hoop stress components due to transverse loading as a function of radial distance from the fibre centre at both 0° and 90° to the loading direction. The stress due to transverse loading is normalized to the maximum applied load. After moulding (Fig. 2a), the hoop, radial, and axial stress in the fibre are compressive; in the matrix the axial stress is zero, the hoop stress is tensile near the fibre, and the radial stress is compressive near the fibre; both are reduced to zero several fibre radii from the interface. After loading to the maximum applied load (Fig. 2b and c), the maximum radial stress is at about 1.42 fibre diameters. The radial stress is negative 90° to the loading direction, but increases to zero some distance away from the fibre. The hoop stress is always positive, and is greatest 90° from the loading direction.

The important feature of these results to note is that the radial stress is the stress that can most easily separate the matrix from the fibre and thus cause the most damage, and the maximum radial stress is not exactly at the fibre-matrix interface, but some distance into the matrix.

3.1.2. Damage due to transverse cycling

A qualitative overview of the transverse cyclic damage process is shown in terms of photoelastic patterns and scanning electron micrographs before the damage to the interphase is presented quantitatively. A series of photoelastic images of the stress transfer zone around a fibre break during the fragmentation test are presented in Fig. 3; both cycled and non-cycled composites are shown. Optical activity is the result of shear stresses in the matrix which develop because of the load transfer from the matrix to the fibre; an absence of optical activity indicates that there is no load transfer. Cyclic damage in the interphase region was measured by a reduction in the average ISS. A reduction in ISS can be seen in the photoelastic patterns as an increase in the length of the stress transfer zone (STZ), and possibly as a reduction in intensity. After cycling at 2.0% and 2.35% strain amplitude (below 10 000 cycles) the fragmentation test revealed that the interphase remained intact in some form as evidenced by optically active regions around a

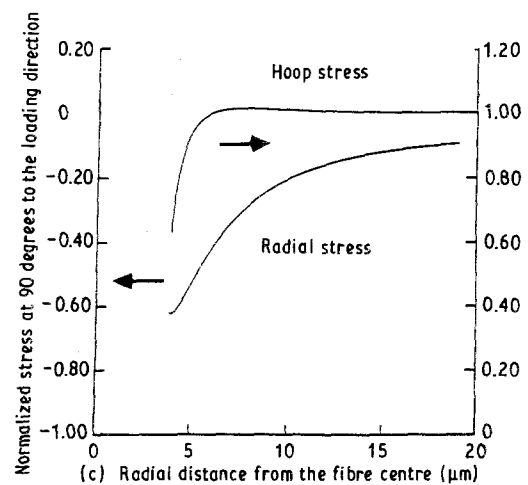
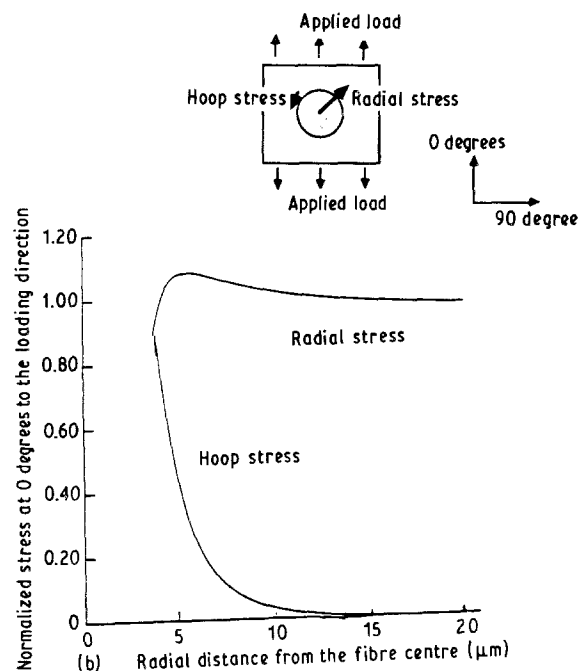
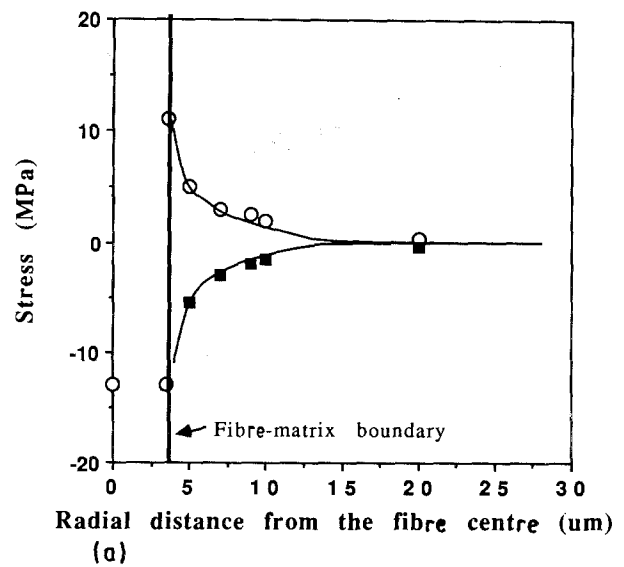


Figure 2 Stress distributions in the composite as a function of radial distance from the fibre centre, (a) in the as-moulded composite (■) radial stress, (○) hoop stress, (b) at 0° to the loading direction at the maximum transverse applied load, (c) at 90° to the loading direction at the maximum applied load. The fibre radius is 3.5 μm.

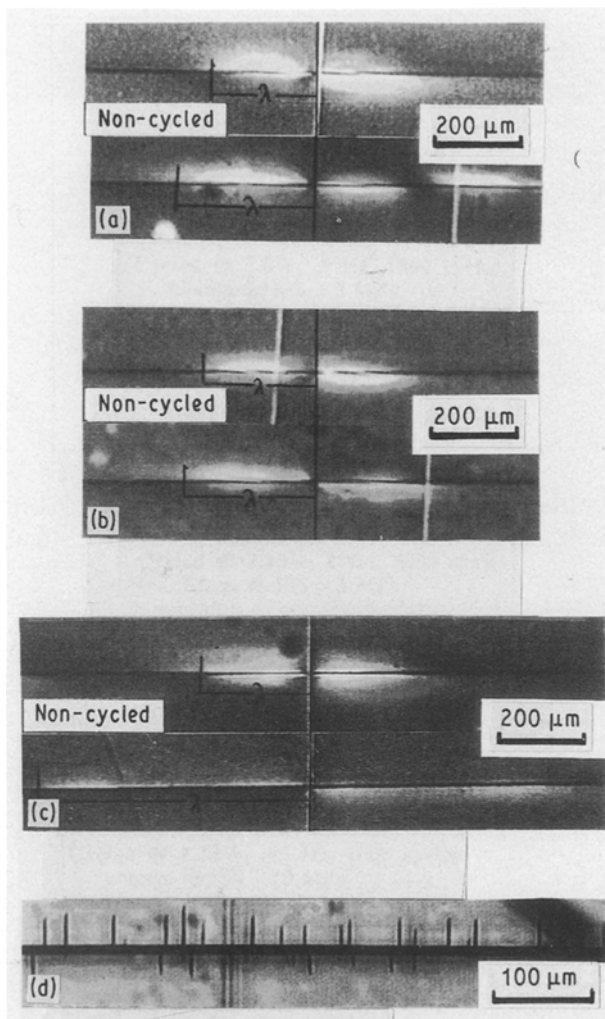


Figure 3 Photoelastic patterns comparing cyclically degraded and non-cyclically single fibres at various degrees of fibre degradation. Change in average ISS; (a) 3 MPa, cycled at 2%, 0.5 Hz, 1500 cycles; (b) 3 MPa, cycled at 2.35%, 1 Hz, 5000 cycles; (c) 10 MPa, cycled at 2.35%, 0.05 Hz, 1000 cycles (d) matrix cracks perpendicular to the matrix when the average ISS = 0.0, cycled at 2.7%, 1000 cycles.

fibre break. The lengthening of the zones is accompanied by a region near the fibre break of lower intensity and constant distance (or zone of influence) into the matrix. When the average ISS changes by 10 MPa, the photoelastic pattern of the cycled sample is much reduced in intensity, and has a constant zone of influence into the matrix for the entire distance along the fibre. After cycling at 2.7% strain amplitude the fragmentation test shows that there was no optical activity near the fibre breaks, and the fibre rarely failed. Instead, optical microscopy revealed an intense bright region around the fibre, and matrix cracks or crazes grew perpendicular to the fibre during the test. The interpretation is that the interphase failed completely during cycling at 2.7% strain creating minute cracks or crazes in the interphase region that then propagated during the fragmentation test.

The locus of failure in the interphase region was observed by pulling the fibres from the matrix and viewing them in a scanning electron microscope. Scanning electron micrographs of both the cycled fibres and the non-cycled fibres pulled from the matrix reveal two noteworthy phenomena (Fig. 4). First, the

samples cycled at 2.35% have failure surfaces similar to the non-cycled samples. This suggests that the interphase has remained intact during cycling, and the mode of failure due to longitudinal testing is similar before and after cycling. Second, at 2.7% strain amplitude, the failure surfaces were not similar to the non-cycled samples; there seem to be large amounts of polycarbonate left on the surface. This indicates that the interphase failed not at the fibre-matrix interface, but some distance away from the fibre in the matrix during cycling. However, the various fracture surfaces of samples cycled at 2.7% are dissimilar, making broader conclusions difficult.

3.1.3. The effect of strain rate

The fatigue properties of bulk polymer composites are known to be dependent on the strain rate of testing [7]. The effect of strain rate on the interphase was investigated by cycling samples from 0.01–1 Hz. At 2.35% amplitude, the degradation of the interphase was found to depend on the strain rate as shown in Fig. 5a–c. The parts of this figure show plots of the change in interfacial shear stress as a function of strain rate for all three sample types. Each sample was cycled at 2.35% strain for 1000 cycles. The slower the strain rate, the greater the degradation in interphase shear stress. The as-received fibre has a greater dependence on strain rate than the 1 or 3 min treated fibres, but any significance to this difference is difficult to determine due to the large error bars.

The change in ISS versus strain rate for samples cycled at 2.0% strain showed no clear dependence of damage on the strain rate, but there was a slight trend towards increased damage at lower strain rates.

A dependence of damage on strain rate was not found at 2.7%, because any evidence was hidden by the complete destruction of the interphase at all frequencies tested.

To test very low strain rates, a creep test was performed at several stress amplitudes. Samples were loaded to the strains reported in Table II, and then the load was held constant. The maximum strain reached during the test, the time of loading, and the reduction in average ISS is reported. The data are somewhat scattered, but the important information to be gained from this table is that even at a strain of 2.8%, the interphase remains intact contrary to the behaviour in the cyclic test. This suggests that the loading and unloading is important for damage accumulation at the interphase.

3.1.4. Damage to the interphase by cycling at 2.0% strain amplitude

2.0% strain amplitude was the lowest strain amplitude used for fatigue testing because even at this high amplitude, the damage to the interphase was found to be minimal. Fig. 6 shows a plot of the post-cyclic average ISS as a function of the initial average ISS. The top 45° line represents the line of zero damage; the lower parallel lines represent a decrease in the average ISS after cycling, in units of 2.5 MPa. The

greatest damage measures about 5 MPa, but most of the damage is less than 4 MPa. The effect of the number of cycles at 0.5 Hz, and at 1.0 Hz is shown in Fig. 7. Damage occurs within the first 1000 cycles at 0.05 Hz, and then reaches a plateau at about 4 MPa. The samples cycled at 1.0 Hz were damaged less than those at 0.05 Hz. Note that all three interphases experience about the same amount of damage, or change in average ISS, even though the initial and final average ISS values differ.

3.1.5. Damage to the interphase by cycling at 2.35 % strain amplitude

To alleviate any question about a crack growing from the edge of the transversely oriented sample while cycling at 2.35 % strain amplitude, several samples

were viewed *in situ* in cross polarization with a travelling microscope; the edge cracks could be seen as optically active zones, but no crack growth was observed during cycling. Damage zones could be seen as zones of photoelastic activity, and were seen to develop during the test from within the sample. The damage at 2.35 % strain amplitude was greater in general than that at 2.0 % as shown in Fig. 8, which shows a plot of the post-cyclic average ISS as a function of the initial average ISS. The observed maximum damage causes up to a 13 MPa decrease in average ISS. The dependence of damage on cycles for 0.05 Hz and 1.0 Hz is shown in Fig. 9. The damage at 0.05 Hz increased rapidly for the first 1000 cycles, and then reached a plateau with an average decrease in average ISS of about 8 MPa. The samples cycled at 1.0 Hz again incurred little damage. Note again that the amount of damage, or the change in average ISS is not dependent on the initial average ISS.

3.1.6. Damage to the interphase by cycling at 2.7 % strain amplitude

After cycling at 2.7 % strain amplitude, the fragmentation test showed that load transfer no longer occurred between the fibre and the matrix; all three types of interphases were destroyed. In many of the fibre interphase regions, matrix cracking or crazing developed perpendicular to the fibre during the fragmentation test. The density of cracks varied along the fibre, and most cracks were no longer than 30 μm , which is

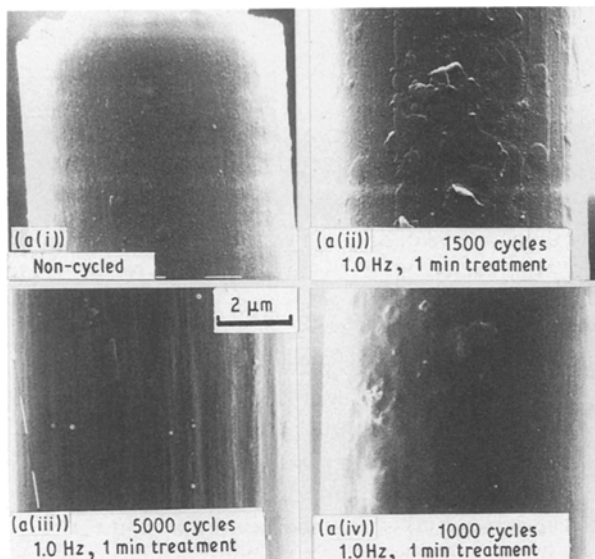
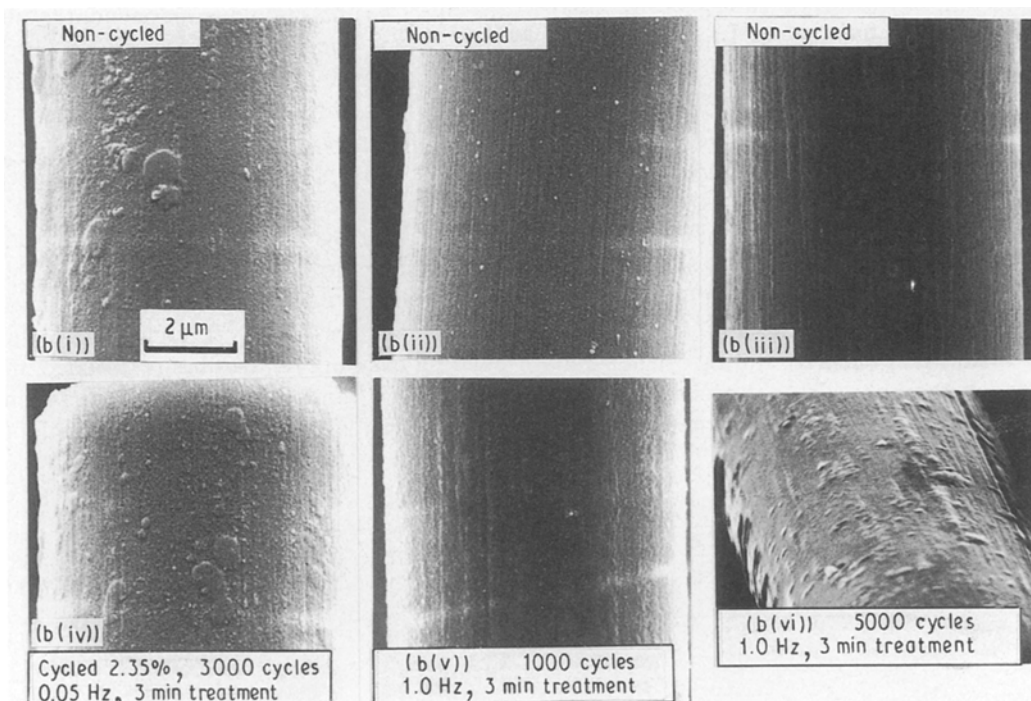


Figure 4 Scanning electron micrographs of AU4 fibres pulled from a polycarbonate matrix before cycling, and after cycling at 2.7 % (except where noted) at the various strain amplitudes indicated: (a) 1 min treated fibres, (b) 3 min treated fibres.



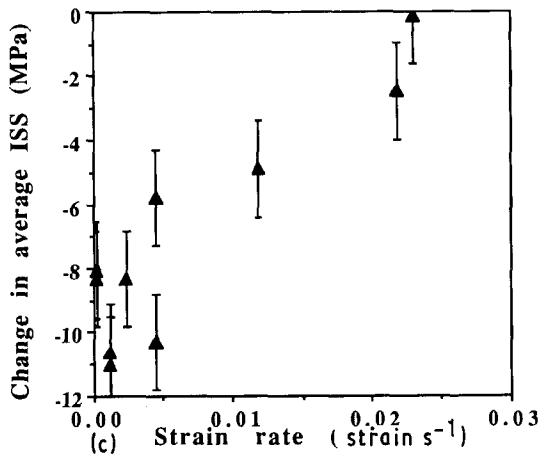
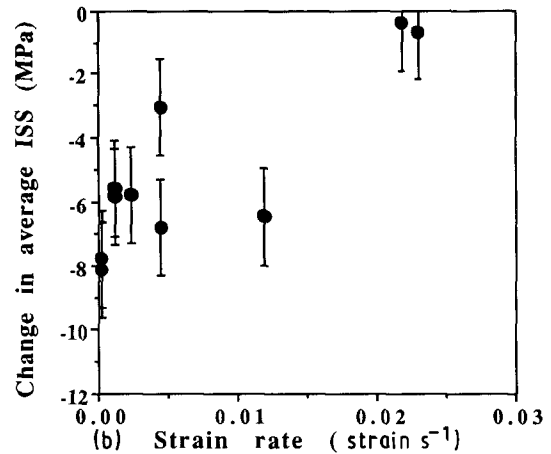
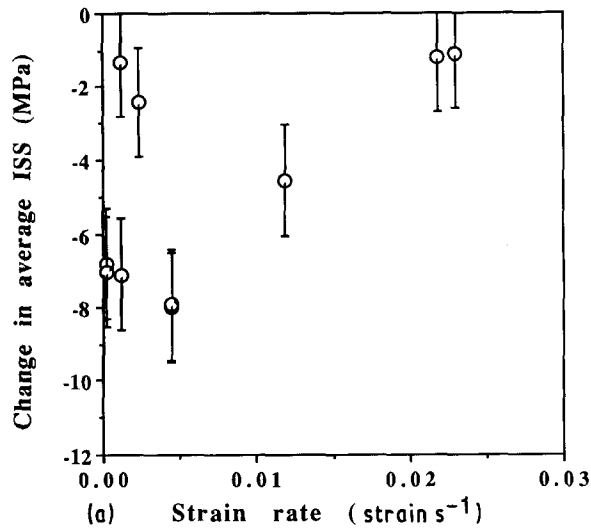


Figure 5 Plots of the change in average interfacial shear stress as a function of strain rate after fatigue at 2.35% strain amplitude, for all three interphase types: (a) 3 min, (b) 1 min, (c) as-received. Each sample was cycled for 1000 cycles.

about the distance that the stress transfer zone extends into the matrix as observed in the photoelastic patterns.

3.2. Axial loading

Two types of interphase were subjected to axial fatigue; because the behaviour was similar for each within the bounds of this investigation, only the results for the fibre treated for 3 min are discussed.

The average ISS was not altered by cycling in the axial direction at strain amplitudes below the failure strain of the fibre, and cycles up to 1×10^6 . At strain amplitudes above the fibre failure strain, two types of damage were observed. The first sample was cycled at 2.4% strain amplitude for 8000 cycles at 0.15 Hz, and the type of damage is exhibited in Fig. 10. The top figure shows breaks that occurred during cycling, and the bottom figure shows breaks that occurred during the fragmentation test. The region of intense photo-

elasticity moved along the fibre during cycling, leaving behind a region of no optical activity. This suggests that complete debonding occurred at the fibre end. The second type of damage was observed in a sample that was cycled at a strain amplitude of 2.8% at 0.01 Hz. The sample was cycled in the mini-tensile tester and was observed *in situ*. The strain amplitude was high enough for the stress transfer zone to extend to the point that there was the typical region of low intensity and then a region of intense optical activity.

The photoelastic patterns shifted during cycling in two ways as shown in Fig. 11. The region of intense optical activity (1) shortened in length, and (2) proceeded along the fibre. Fig. 12 follows the development of the photoelastic patterns during one cycle of the test. Fig. 12b shows a schematic illustration of the shear in the interphase and the strain distribution in the fibre. As the sample is unloaded, the fibre end is under some compression because the fibre is being forced back into the cylinder it slide out from, and the cylinder has since shrunk in size due to Poisson's effects. The region of compression grows as the fibre unloads until the minimum strain is reached. At the minimum strain the fibre is not under zero load, but there are two regions of shear: the region near the fibre end in which the fibre is decreasing in load, so the sign of the shear is negative, and the region closer to the end of the stress transfer zone where the load is building back up. As the fibre is reloaded, the load at the fibre end builds, but the region in between is still at a lower strain; therefore, there is an additional change

TABLE II The change in the average ISS for each fibre type due to transverse creep

Strain amplitude %	Maximum strain reached	Time (h)	Change in ISS for 3 min treatment (MPa)	Change in ISS for 1 min treatment (MPa)	Change in ISS for as-received fibres (MPa)
1.85	2.1	9.0	9	6	7
2.1	2.35	22.5	6	5.5	5
2.8	3.24	7.0	5	5	7

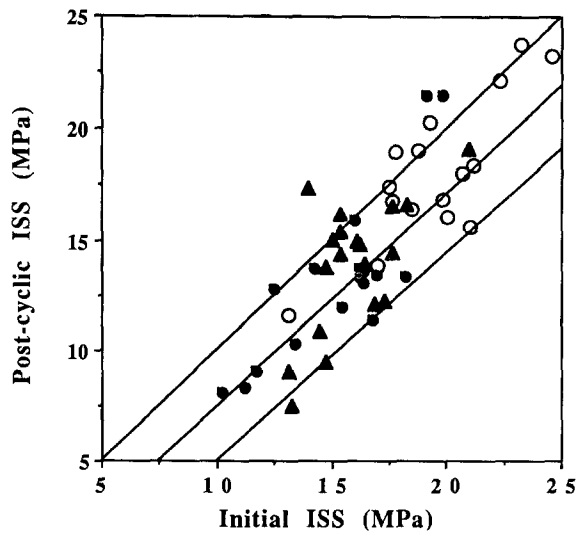


Figure 6 A plot of the post-cyclic average ISS versus the initial average ISS for samples at a strain amplitude of 2.0%. The upper 45° line represents the line of zero damage. Lower lines are at intervals of 2.5 MPa. (○) 3 min treatment, (●) 1 min treatment, (▲) as-received.

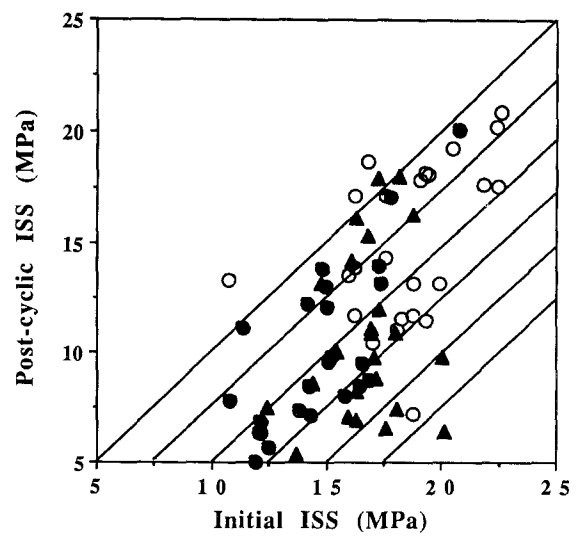
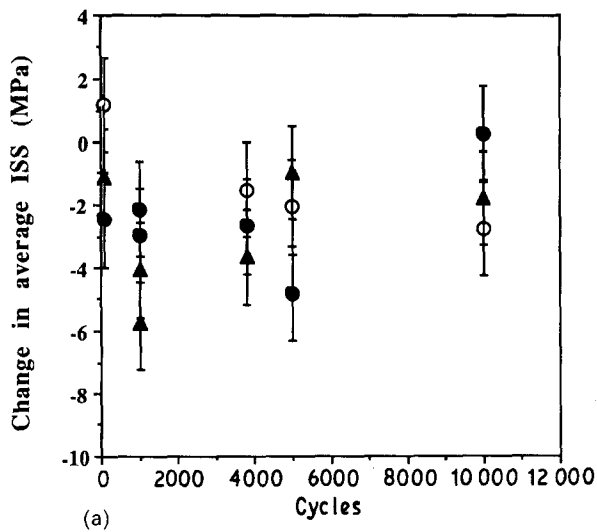
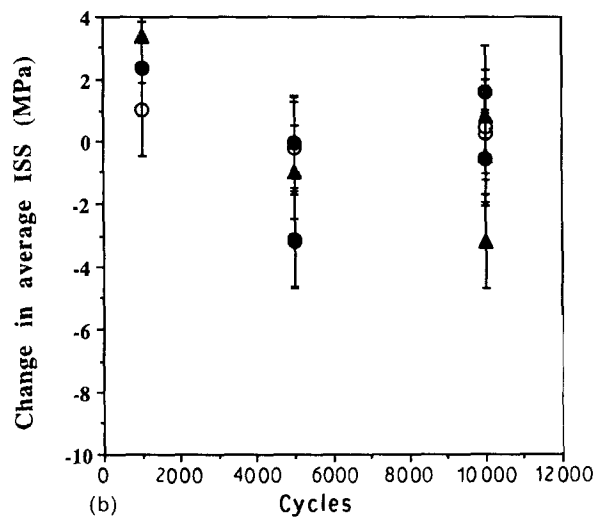


Figure 8 A plot of the post-cyclic average ISS versus the initial average ISS for samples cycled at a strain amplitude of 2.35%. The upper 45° line represents the line of zero damage. Lower lines are at intervals of 2.5 MPa. (○) 3 min treatment, (●) 1 min treatment, (▲) as-received.

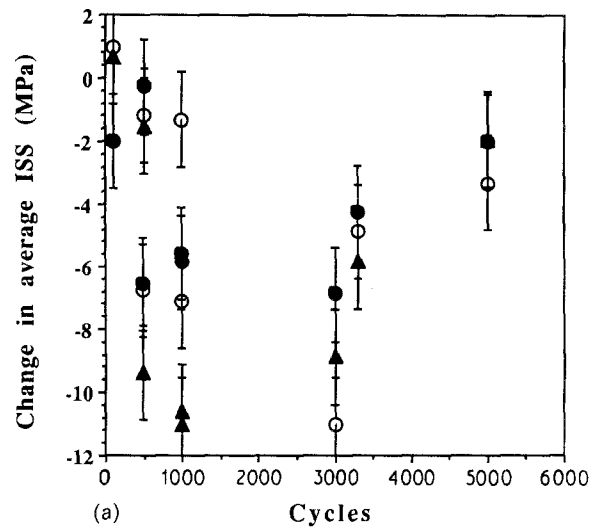


(a)

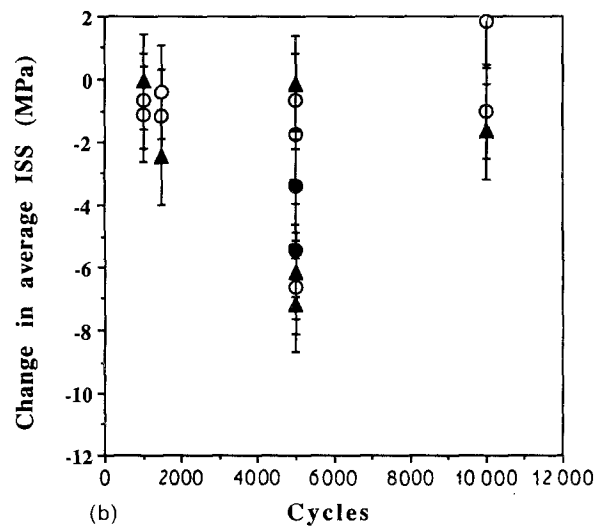


(b)

Figure 7 Change in the average interfacial shear stress as a function of cycles at 2.0% strain amplitude at two different frequencies: (a) 0.05 Hz, (b) 1.0 Hz. (○) 3 min treatment, (●) 1 min treatment, (▲) as-received.



(a)



(b)

Figure 9 Change in the average interfacial shear stress as a function of cycles at 2.35% strain amplitude for two different frequencies: (a) 0.05 Hz, (b) 1.0 Hz. (○) 3 min treatment, (●) 1 min treatment, (▲) as-received.

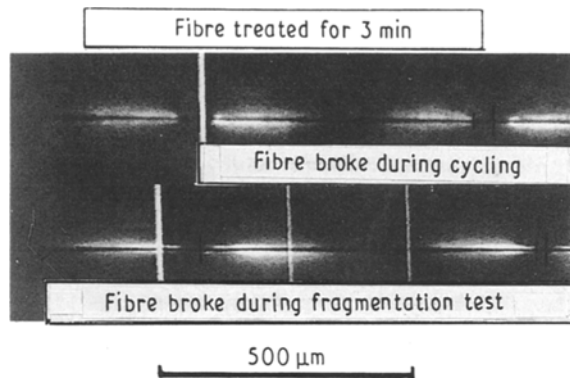


Figure 10 Photoelastic responses of a fibre cycled for 8000 cycles at a strain amplitude of 2.5 % at 0.15 Hz. The top figure shows breaks that occurred during cycling and the bottom figure shows breaks that occurred during the fragmentation test.

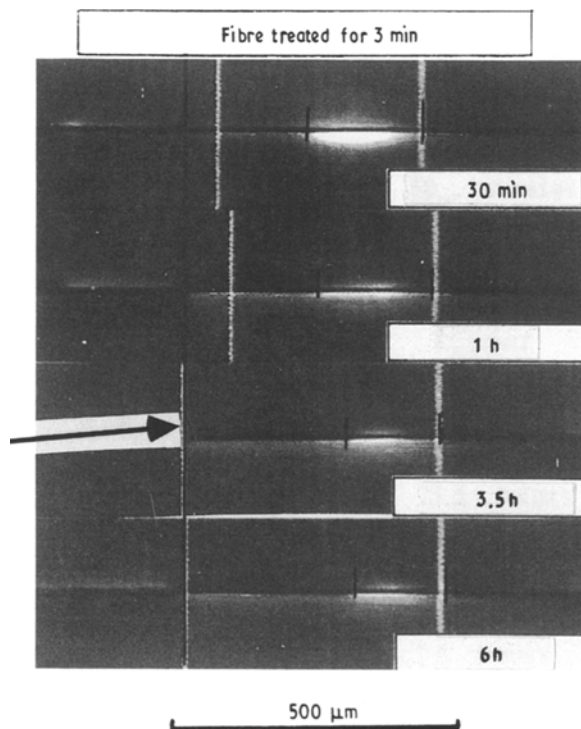


Figure 11 The development of the photoelastic pattern in the stress transfer zone with time as the sample is cycled axially.

in the sign of the shear. The end continues building in load, the next region shows a decline in load because of the compressive load introduced during unloading, and then there is an increase in load because the middle regions of the fibre remain at a higher strain than the fibre end.

4. Discussion

4.1. Transverse fatigue

It is well known that polycarbonate softens considerably during tension/compression cyclic loading [8]. The fatigue tests run in this work were tension-tension tests with $R = 0.1$ and were run under load control; no macroscopic softening was observed during cycling. In fact, the sample hardened slightly. This may be due to the low cyclic strain or because the stress was always tensile. However, the interphase was cycled from tension to compression. The residual

radial stress in the matrix surrounding the fibre at zero load is -15 MPa. During cycling the radial stress at the poles of the fibre reach a maximum tensile stress of 1.1 times the applied load as shown in Fig. 2. The interphase at 90° to the loading direction remains in radial compression during the entire test. The portion of the interphase that is cycled from tension to compression may experience the softening behaviour usually observed in polycarbonate [8]. If this is so, then the following sequence of events could lead to the damage observed in the interphase.

At the lowest strain amplitude, the macroscopic composite is at 32 MPa. The region at the poles of the interphase was therefore cycled from about 35 to -10 MPa, and presumably softened during cycling. Because softening is accompanied by an apparent loss of modulus, the modulus of the interphase is lower. A lower modulus results in a lower average ISS because the load transfer is controlled by the axial displacement difference (shear lag) between the matrix and the fibre [9]. For a given difference in displacement, materials with a lower modulus will transfer less load, and therefore less strain to the fibre. The fibre strain is equal to the shear stress integrated over the distance from the fibre end. If the shear stress is lower, the length of the stress transfer zone increases to transfer the same amount of load. There is no apparent debonding at the interphase, as evidenced by the similar scanning electron micrographs between non-cycled and cycled pull-out fibres. The plateau in damage is reached because polycarbonate softens, and then has a long period of stability before any failure occurs. There may be an additional mechanism of stress relief in the interphase region during cycling.

The sample cycled at 42 MPa, and at a strain amplitude of 2.7 %, also is considered to soften. However, at this high load, the sample is above the cyclic yield stress, and the material yields to failure during testing. The failure may begin at the poles of the fibre, but then proceeds around the fibre. The failure occurs at some distance into the matrix because the highest stress occurs at about 1.42 times the fibre radius. Subsequent cycling results in wear between the two materials. The matrix cracking (or crazing) during the fragmentation test is presumably caused by flaws generated during cycling that propagate into the softened region. The length of the crack is limited to the affected zone.

The sample cycled at the intermediate strain amplitude experiences some combination of the effects described above. There is a large reduction in the average ISS, and the photoelastic patterns are of low intensity, and of constant intensity for a long distance along the fibre. They resemble the photoelastic patterns observed at high strains in the monotonic fragmentation tests. This type of photoelastic pattern is indicative of a frictional load transfer because a frictional mechanism of load transfer is characterized by an ISS that is low and approximately constant within the STZ. The ISS would translate into photoelastic patterns that are of low intensity extended along the fibre. A frictional mechanism of load transfer implies that the interphase has failed. Scanning electron

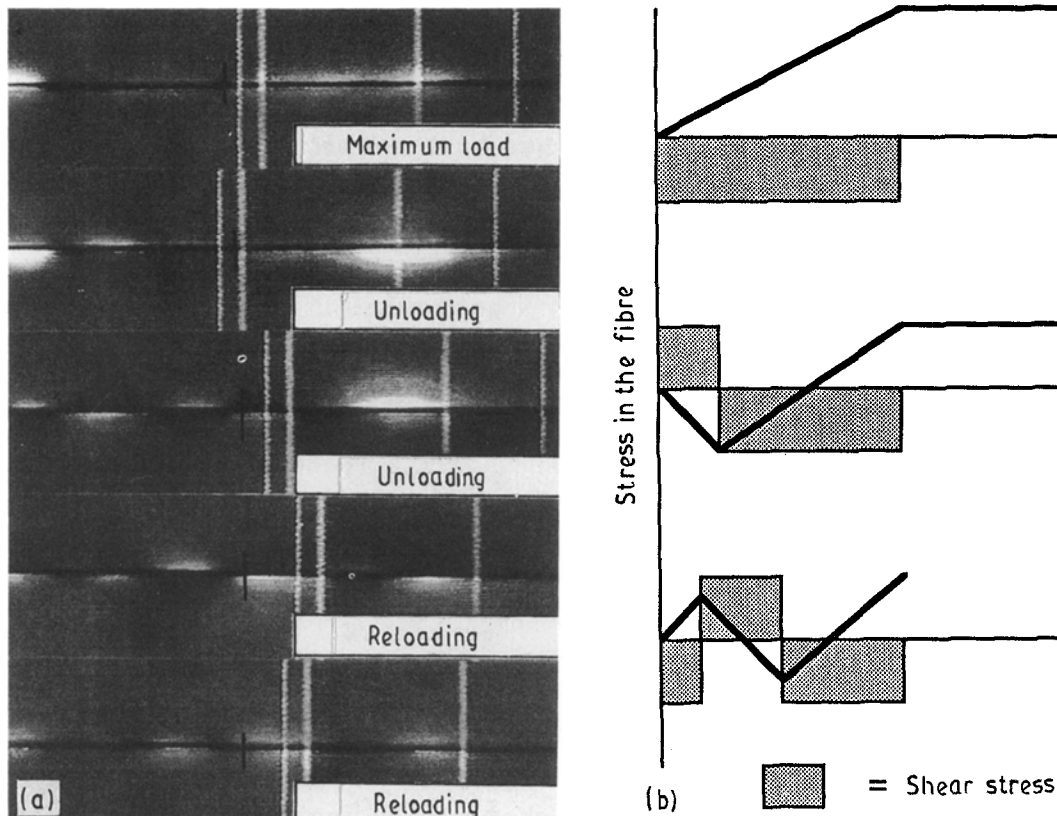


Figure 12 The development of the photoelastic pattern in the stress-transfer zone as the fibre is unloaded and reloaded. (a) Photoelastic patterns, (b) schematic illustration of the strain in the fibre, and the shear in the interphase.

micrographs of the fibre surface of a fibre pulled from a cycled sample look the same as a fibre pulled from a non-cycled sample; this indicates, however, that complete failure has not occurred in the interphase during cycling as in the samples cycled at 2.7%. It may be that the matrix in the interphase region has been weakened such that when the fibre breaks, the same type of debonding that occurs in high strains in the monotonic samples, occurs at lower strains yielding a frictional mechanism of load transfer at lower strains.

An important feature of these results is that the same amount of damage was observed in all three types of interphase. This suggests that the interphase behaviour is matrix dominated. This is congruent with the behaviour observed in static loading reported in Part I of this report. The increase in the average ISS associated with loading in the axial direction is due to an enhanced surface roughness, and nominally an increased shear strength of the fibre surface. In the direction normal to the fibre surface, these properties do not exert as much of an influence; the damage in the radial direction is dependent on the radial properties, and is therefore insensitive to an increase in fibre roughness.

4.2. Strain-rate effects in transverse fatigue

Recently, it was found that the lifetime of polycarbonate is dependent on frequency over a strain rate range of 1×10^{-3} – 10 [10]. At strain rates less than 1×10^{-2} , a craze mode of crack growth prevailed, and the total number of cycles to failure was constant. This suggests that loading and unloading is more important in

determining lifetime than creep, because the total time to failure is not the determining feature; it is the number of cycles. The data in this report are congruent with that conclusion. Creep tests at strains as high as 2.8% did not exhibit as much damage as samples cycled at 2.7%.

At strain rates from 1×10^{-2} – 1×10^{-1} , the lifetime of polycarbonate increases, and shear begins to play a greater role in crack growth creating the well-known epsilon-shaped crack zones [10]. The strain rates when cycling at 1–10 Hz were 1×10^{-2} – 1×10^{-1} . The strain rate for the samples cycled at 2.35% at 1 Hz is about 2×10^{-2} . Therefore, the samples cycled in this study at 1 Hz should exhibit the expected increase in lifetime. A close look at the damage to the interphase versus strain rate plot in Fig. 5 reveals that the largest drop in damage after 1000 cycles at 2.35% occurs in the range from 1.0×10^{-2} – 2.0×10^{-2} . The damage at the interphase follows closely the damage in a bulk polycarbonate sample, supporting previous evidence suggesting that cyclic damage induced by transverse loading is matrix dominated.

4.3. Axial loading

Cyclic damage was not introduced into the interphase at axial strain amplitudes below the failure strain of the fibre because the shear stress in the interphase was zero. The shear stress was zero because the fibre was very long, and the region examined was far from the fibre end. The radial, hoop and axial stresses were less than 2.0%, which is almost within the “linear” region of polycarbonate behaviour. Once the strain amplitude was high enough to fail the fibre, there were

regions of shear near the fibre end (stress transfer zones), and there was a large stress concentration surrounding the fibre break; these resulted in two types of damage to the interphase region. In both types of damage, the stress transfer zone moved along the fibre. In the first case the damage was concentrated around the fibre break. Consider the crack near the fibre end with a length β along the fiber, and α perpendicular to the fibre. If β is small, then damage will be concentrated near the fibre end as in Fig. 10. If β is large, the crack along the fibre reduces the stress concentration at the fibre end, and concentrates it instead in the stress transfer zone. This phenomenon, which was observed, caused the stress transfer zone to grow; the length of the region of intense load shrunk because load was carried through friction in the region of the extended crack, and the amount of load that needed to be transferred, decreased.

Axial fatigue has also been performed on AU4/J2[®] samples [11]. The as-received AU4 fibres in J2[®] behaved in much the same way as the AU4 fibres in polycarbonate, but the treated fibres in J2[®] behaved differently from those in polycarbonate. If the axial fatigue strain was high enough to fail the treated fibres, the cracks that were formed when the fibre broke were matrix cracks perpendicular to the fibre. The cracks grew perpendicular to the fibre with cycles, until eventually they became shear bands and grew at 45° to the loading direction. The mono-filament composites failed because of the growth of these cracks.

It is clear from the above behaviour that the interphase will strongly affect the fatigue properties of a bulk composite, especially in the case of multi-axial loading. If the interphase is tougher than the matrix as in the case of treated fibres in J2[®], fibre breaks will cause a crack to grow into the matrix perpendicular to the fibre. Little fibre pull-out will occur, and the result will be a brittle type of fracture. However, the strength of the interphase may be reduced during cycling, such that the crack surrounding a fibre break may proceed along the interphase. This would increase the amount of fibre pull-out, and increase the crack growth resistance of the composite.

The fatigue behaviour of the interphase is also affected by the matrix. First, although the absolute value of the interphase strength will be affected by the initial conditions of the interphase, the amount of damage due to transverse cycling will depend on the matrix properties. In addition, the interphase in the composites with treated AU4 fibres behaved differently in J2[®] than in polycarbonate. J2[®] is a weaker, less tough matrix, and the stronger interphase in the treated fibres resulted in matrix cracking which would reduce the composite toughness. From the above data it is clear that interphases must be carefully tailored to produce optimal composite lifetime taking into consideration both matrix and interphase properties.

5. Conclusions

Experiments on the transverse and axial fatigue of mono-filament composites lead to the following conclusions.

1. The damage in the interphase of an AU4/PC mono-filament composite cycled in the transverse direction is matrix dominated. Although the change in average ISS does not depend on the type of interphase indicating the influence of the matrix, the absolute value of the average ISS is mediated by the fibre surface.

2. Damage in AU4/PC composites is characterized by matrix softening at low strain levels (2.0%), an overall weakening of the matrix surrounding the fibre at higher strain amplitudes (2.35%), and at strain amplitudes above 2.7% failure occurs during cycling in the matrix region of the interphase.

3. The fatigue behaviour of the interphase in a mono-filament composite cycled in the axial direction is dependent on the filament strength because there is no damage in the fibre until the strain amplitude is greater than the failure strain of the fibre.

4. After a fibre has fractured during axial fatigue, a complicated state of stress develops around the fibre break resulting in damage to the interphase characterized by a growth of the stress transfer zone, and debonding in the stress transfer zone.

Acknowledgements

The work was supported jointly by the E. I. Du Pont de Nemours and Co Inc., and by the University of Pennsylvania under the auspices of the Laboratory for Research on the Structure of Matter (Composites interface thrust). The work was further promoted by the generous advice and assistance of A. L. Radin and D. Ricketts, University of Pennsylvania, and L. Peterson and B. Campbell, E. I. Du Pont de Nemours and Co Inc.. Discussions with Z. Hashin were very helpful.

References

1. R.C. TENNYSON, T. A. WATERHOUSE, S. NEWMAN and M.T. TAKEMORI, *Polym. Compos.* **6** (1982) 437.
2. F.J. McGARRY and M. FUJIWARA, in "Proceedings of the 23rd Annual Technical Conference", Reinforced Plastics Division (SPI, 1968).
3. A. T. DIBENEDETTO, L. NICOLAIS, L. AMBROSIO and J. GROEGER, in "Proceedings of the First International Conference on Composite Interfaces (ICCI-I)", Cleveland, OH, 1986, edited by H. Ishida and J. L. Koenig (Elsevier Science, New York, 1986).
4. L. T. DRZAL, *Adv. Polym. Sci.* **75** (1986) 1.
5. L. S. SCHADLER, J. C. FIGUEROA and C. LAIRD, in "Proceedings of the Materials Research Society", Vol. 170, November 1989, edited by C. G. Pantano and E. J. H. Chen (Materials Research Society, Pittsburgh, PA, 1989) p. 345.
6. J. C. FIGUEROA, L. S. SCHADLER and C. LAIRD, *ibid.*, p. 65.
7. R. W. HERTZBERG and J. A. MANSON, "Fatigue of Engineering Plastics" (Academic Press, New York, 1980).
8. P. BEARDMORE, "Treatise on Materials Science and Technology", Vol. 6 (Academic Press, New York, 1975).
9. A. KELLY and W. R. TYSON, *J. Mech. Phys. Solids* **13** (1965) 329.
10. M. T. TAKEMORI, *Polym. Engng Sci.* **27** (1987) 1.
11. J. C. FIGUEROA (1990) private communication.

Received 16 January
and accepted 17 May 1991